The Mean Excitation Energies and Their Directional Characteristics for Energy Deposition by Swift Ions on the DNA and RNA Nucleobases

ARTICLE *in* THE JOURNAL OF PHYSICAL CHEMISTRY C · NOVEMBER 2012

Impact Factor: 4.77 · DOI: 10.1021/jp1021054

3 AUTHORS:

Stephan P. A. Sauer
University of Copenhagen
179 PUBLICATIONS **3,582** CITATIONS
SEE PROFILE

Jens Oddershede
University of Southern Denmark
192 PUBLICATIONS **5,236** CITATIONS
SEE PROFILE

John R. Sabin
University of Florida
163 PUBLICATIONS **1,619** CITATIONS
SEE PROFILE

Mean Excitation Energies and Their Directional Characteristics for Energy Deposition by Swift Ions on the DNA and RNA Nucleobases[†]

Stephan P. A. Sauer,[‡] Jens Oddershede,[§] and John R. Sabin*[,§]

Department of Chemistry, University of Copenhagen, Copenhagen, Denmark, Department of Physics and Chemistry, University of Southern Denmark, Odense, Denmark, and Quantum Theory Project, Department of Physics, University of Florida, Gainesville, Florida

Received: March 8, 2010; Revised Manuscript Received: April 22, 2010

As the mean excitation energy of a molecule is the materials parameter that describes the energy transfer from a swift ion to a molecule, knowledge of it and its properties are necessary to an understanding of ion−molecule interactions. A particularly important case is the interaction of fast ions with biological material. In this contribution we calculate the mean excitation energies of the nucleobases using the polarization propagator formalism. The mean excitation energies and their directional components are calculated, as are the influence of hydrogen bonding and nucleoside formation. We find that the mean excitation energies of the five nucleobases are remarkably similar, but sensitive to the orientation of the target base with respect to the ion beam direction. The mean excitation energies are also very stable with respect to hydrogen bonding and nucleoside formation.

1. Introduction

Understanding the basic physics of the interaction of radiation with biological targets becomes ever more important as we seek to protect healthy cells from radiation damage and to target therapeutic radiation (e.g., in the form of proton or C^{6+} ion beams[1,2]) selectively on pathologic cells. The problem extends over many orders of magnitude in complexity, time scale, and size as the effects of the interaction of radiation with matter become more complicated. For example, the time scales for bioradiological processes begin with attoseconds and continue through tens of years (e.g., the Nagasaki studies[3,4]). The problem of describing and understanding the effects of radiological action on biological systems is thus exceedingly complicated, as one must describe long chains of sequential and parallel chemical and physical events, as well as possible nonlinearities between initial radiogenic molecular changes and final biological effects.[5−7] The chain of events can be viewed in a hierarchical scheme beginning with the initial interaction of the radiation with a molecule in a biological sample. All of the involved processes must be well-understood to deal effectively with problems such as radiation protection and radiation therapy. However, in all cases, the understanding and description of radiological action on biosystems begin with the determination of the energy deposited.

The major biological damage resulting from the exposure of cells to radiation comes from either single (SSB) or double (DSB) strand breaks in DNA and, to a lesser extent, from damage to intracellular proteins. Although a minority of damage is produced by direct hits of ions on either DNA or proteins, energy deposition by a fast ion in direct collision with a biomolecule, and the subsequent excitation and fragmentation of the target, must be understood. In our work, we are therefore concerned with the first step in this process, namely, the energy transfer consequences of swift ions impinging on biomolecules.

Massive particles, as opposed to photons, deposit energy in a molecule by collision with either the electrons (the dominant mechanism) or the nuclei of the molecule. The collision typically results in electronic excitation of the target molecule, followed by some combination of ionization, decay, emission of secondary radiation, or fragmentation. The energy deposition depends on the electronic structure of the target system and its propensity to absorb energy from a swift projectile. The material constant of the target that quantifies energy absorption within the simplest version of the Bethe theory[8,9] is the mean excitation energy. The mean excitation energy of a target is thus a parameter that is very helpful to know before making theoretical predictions or planning experiments, regardless of the theory or model used.

In previous studies we have investigated the mean excitation energy of the molecule which is ubiquitous in all biological systems, that is, the water molecule,[10,11] as well as of amino acids and small peptides.[12−16] For the latter we have in particular studied the importance of different conformations,[12,16] the orientation of the molecules with respect to the incoming beam,[12,16] and the influence of the surrounding water molecules.[14] In the present study we turn now to DNA or RNA and their constituent nucleobases: adenine, cytosine, guanine, thymine, and uracil.

2. Bethe−Born Theory of Energy Deposition by Swift Ions

Energy transfer to a molecule by a fast ion is frequently described in terms of the so-called linear energy transfer (LET), or stopping power $-\mathrm{d}E/\mathrm{d}x$, of the target molecule.[9,17,18] To avoid problems when comparing stopping in targets of different densities, one frequently considers the stopping cross section $S(v)$:

[†] Part of the "Mark Ratner Festschrift".
* Corresponding author.
[‡] University of Copenhagen.
[§] University of Southern Denmark and University of Florida.

10.1021/jp1021054
Published on Web 06/02/2010

$$-\frac{dE}{dx} = nS(v) \tag{1}$$

where n is the number density of the scatterers and v is the projectile velocity. The cross section is further written in terms of the stopping number, $L(v)$, as:

$$S(v) = \frac{4\pi e^4 Z_1^2 N_e}{mv^2} L(v) \tag{2}$$

Here Z_1 and N_e are the projectile charge and target electron number, respectively. The simplest version of stopping theory, which we employ here, the Bethe theory and using the dipole approximation, is valid for conditions where the projectile velocity is much larger than that of the target electrons. This leads to the simplest form of the stopping number, which can be written:

$$L(v) = \ln \frac{2mv^2}{I_0} - \frac{C(v)}{N_e} \tag{3}$$

The rightmost term in eq 3 is referred to as the shell corrections, and it is present to compensate for cases where the projectile velocity is not considerably larger than the target electron velocity, as is assumed in the Bethe theory. At a large projectile velocity, the shell corrections consequently approach zero. The quantity I_0 is known as the mean excitation energy of the target and is defined as the first energy weighted moment of the dipole oscillator strength distribution (DOSD) of the target

$$\ln I_0 = \frac{\sum_k^{\text{bound}} f_{0k} \ln E_{0k} + \int^{\text{continuum}} \ln E_{0k} \frac{df_{0k}}{dE_{0k}} dE_{0k}}{\sum_k^{\text{bound}} f_{0k} + \int^{\text{continuum}} \frac{df_{0k}}{dE_{0k}} dE_{0k}} = \frac{L_0}{S_0} \tag{4}$$

Here $\{E_{0k}\}$ is the complete set of electronic excitation energies for the target, $E_{0k} = E_k - E_0$, and $\{f_{0k}\}$ is the complete set of the corresponding dipole oscillator strengths, which, in the dipole length formulation and Hartree atomic units, is defined as:

$$f_{0k} = \frac{2}{3}(E_k - E_0)|\langle\Psi_0| \sum_i \hat{\mathbf{r}}_i |\Psi_k\rangle|^2 \tag{5}$$

If the square of the norm is "interpreted" as the dot product of the indicated matrix element and its adjoint, then eq 5 represents the oscillator strength of the directionally averaged dipole oscillator strength. For the dipole oscillator strength for that direction, then the coordinate in the average value should be that direction, and the prefactor should be 2.

In the exact limit and certain approximate methods, the dipole oscillator strength sum fulfills Thomas−Reiche−Kuhn (TRK) sum rule as follows[19−21]

$$S_0 = \sum_k^{\text{bound}} f_{0k} + \int^{\text{continuum}} \frac{df_{0k}}{dE_{0k}} dE_{0k} = N_e \tag{6}$$

which expresses that the sum over the complete set of dipole oscillator strengths of the target should equal the number of electrons N_e in the target molecule.

Using individual Cartesian components of the dipole moment operator $\sum_i \hat{\mathbf{r}}_i$ in eq 5, we can obtain directional components I_0^x, I_0^y, and I_0^z of the mean excitation energy from eq 4, which are related to their mean value as

$$I_0 = (I_0^x I_0^y I_0^z)^{1/3} \tag{7}$$

Furthermore, one can define an anisotropy A in the energy deposition[11] arising from the relative orientation of the projectile direction with respect to the plane of the nucleobase. The mean excitation energy and thus the stopping cross section of an anisotropic target depend only on electronic transitions with the polarization direction perpendicular to the direction of the projectile.[22] The anisotropy A is consequently defined in terms of the directional components as

$$A = -N_e \ln \frac{I_0^x I_0^y}{(I_0^z)^2} = -N_e \ln \frac{I_0^{\parallel}}{I_0^{\perp}} \tag{8}$$

Since we will place the plane of the nucleobases in the xy-plane we will have that the projectiles moving in the plane of the base are described by I_0^x and I_0^y, while those moving perpendicular to the plane of the nucleobases are described by I_0^z. The symbols $\perp$ and $\parallel$ refer thus to the orientation of the projectile beam with respect to the molecular plane.

Inokuti et al. pointed out[23] that "the mean excitation energy, I_0, is the sole nontrivial property of matter appearing in Bethe's expression for the stopping power for a charged particle at high speed." The mean excitation energy measures the difficulty with which a target molecule can absorb energy from a massive projectile. Large mean excitation energies correspond to greater difficulty for the absorption of energy by a target molecule and thus lead to lower stopping power. We will thus concentrate on the mean excitation energies of the nucleobases as descriptors of their interaction with swift ions.

3. Dipole Oscillator Strength Distributions Obtained from Polarization Propagators

The vertical electronic excitation energies and associated electronic transition dipole moments for a molecule can conveniently be extracted from the linear response function or polarization propagator,[24] as can be seen from its spectral representation in the basis of the eigenstates $\{|\Psi_0\rangle, |\Psi_k\rangle\}$ of the molecular Hamiltonian $\hat{H}$:

$$\langle\langle \hat{P}; \hat{Q} \rangle\rangle_E = \sum_{k\neq 0} \left[\frac{\langle\Psi_0|\hat{P}|\Psi_k\rangle\langle\Psi_k|\hat{Q}|\Psi_0\rangle}{E - E_k + E_0} + \frac{\langle\Psi_0|\hat{Q}|\Psi_k\rangle\langle\Psi_k|\hat{P}|\Psi_0\rangle}{E + E_k - E_0} \right] \tag{9}$$

where the sum is over all excited states $\{|\Psi_k\rangle\}$ of the system. The poles and residues of the propagator give thus the excitation energies, $E_{0k} = E_k - E_0$, and transition matrix elements, $\langle\Psi_0|\hat{P}|\Psi_k\rangle$, of the operators $\hat{P}$ and $\hat{Q}$. If we choose $\hat{P} = \hat{Q} = \sum_i \hat{\mathbf{r}}_i$, then the residues and poles may be used to compute the dipole oscillator strengths of the system in the length formulation, (all

quantities are in Hartree atomic units), while choices of $\hat{P} = \hat{Q} = \sum_i \hat{\mathbf{p}}_i$ or $\hat{P} = \sum_i \hat{\mathbf{r}}_i$ and $\hat{Q} = \sum_i \hat{\mathbf{p}}_i$ lead to dipole oscillator strengths in the velocity and mixed formulations, respectively.

However, to obtain excitation energies and transition moments from the polarization propagator, one cannot use the spectral representation in the eigenbasis of the Hamiltonian, eq 9, but has to start from a nondiagonal matrix representation

$$\langle\langle \hat{P};\hat{Q}\rangle\rangle_E = \tilde{\mathbf{T}}^{[1]}(\hat{P})(E\mathbf{S}^{[2]} - \mathbf{E}^{[2]})^{-1}\mathbf{T}^{[1]}(\hat{Q}) \qquad (10)$$

where $\mathbf{E}^2$ and $\mathbf{S}^2$ are the molecular Hessian and overlap matrix

$$(\mathbf{E}^{[2]})_{ij} = \langle\Psi_0|[h_i, [\hat{H},h_j^\dagger]]|\Psi_0\rangle \qquad (11)$$

$$(\mathbf{S}^{[2]})_{ij} = \langle\Psi_0|[h_i, h_j^\dagger]|\Psi_0\rangle \qquad (12)$$

and $\tilde{\mathbf{T}}^{[1]}(\hat{P})$ and $\mathbf{T}^{[1]}(\hat{Q})$ are property gradient vectors

$$(\tilde{\mathbf{T}}^{[1]}(\hat{P}))_i = \langle\Psi_0|[\hat{P},h_i]|\Psi_0\rangle \qquad (13)$$

$$(\mathbf{T}^{[1]}(\hat{Q}))_i = \langle\Psi_0|[h_i^\dagger,\hat{Q}]|\Psi_0\rangle \qquad (14)$$

Choosing the operators $\{h_i\}$ to be the state transfer operators $\{|\Psi_k\rangle\langle\Psi_0|;|\Psi_0\rangle\langle\Psi_k|\}$ would lead us back to the spectral representation, eq 9. In practical applications, however, the exact ground state of the system $|\Psi_0\rangle$ is replaced by some approximate wave function $|\Phi\rangle$ which is a linear combination of antisymmetrized products of molecular orbitals, so-called Slater determinants, while the operators $\{h_i\}$ replace one or more of the occupied molecular orbitals by virtual orbitals in the Slater determinants or virtual orbitals by occupied orbitals. Approximations to the vertical electronic excitation energies E_{0k} are then obtained by solving the eigenvalue problem

$$(\mathbf{E}^{[2]} - E_{0k}\mathbf{S}^{[2]})\mathbf{X}_{0k} = 0 \qquad (15)$$

and the corresponding approximations to the transition matrix elements are calculated from the eigenvectors $\mathbf{X}_{0k}$ as

$$\langle\Psi_0|\hat{P}|\Psi_k\rangle = \tilde{\mathbf{T}}^{[1]}(\hat{P})\mathbf{X}_{0k} \qquad (16)$$

This approach yields a finite number of excitations. As a result, the integrations over the continnum states in eqs 4 and 6 are done numerically using the excitation energies with energies larger than the first ionization energy of the system, called pseudostates, as integration points. We have found that this discretization of the continuum works well when sums over the entire excitation spectrum are taken.[25] It should be noted that energy weighted oscillator strength sums can also be obtained directly from matrices used in the polarization propagator,[26,27] but the direct sum over states was used in this application as it was more convenient. The DOSD sum rules and mean excitation energies in eq 4 are then obtained by explicit summation of the oscillator strengths to all bound states and to the discrete continuum pseudostates. In a previous study on alanine,[16] we found that about 12% of the mean excitation energy is due to excitation to bound states, while the remaining 88% comes from transitions into the pseudostates.

Different types of reference wave functions $|\Phi\rangle$ and corresponding sets of excitation operators $\{h_i\}$ can be employed in eqs 11 and 12. Experience shows[10,11] that some amount of electron correlation is needed to calculate reliable spectral moments of the DOSD. One needs to calculate the propagator at least at the level of the time-dependent Hartree−Fock, also called the random phase approximation (RPA),[28,29] which implies using a Hartree−Fock self-consistent field wave function as reference wave function $|\Phi\rangle$ and restricting the excitation operators $\{h_i\}$ to the excitations from a single occupied molecular orbital to one virtual molecular orbital or vice versa. The RPA adds correlation in both ground and excited states in a balanced way.[30] It should be noted that in the RPA used here the dipole oscillator strengths calculated in dipole velocity, dipole length, or mixed representation and all sum rules would be identical and the TRK sum rule, eq 6, would be fulfilled exactly, that is, equal to the number of electrons, if the computational basis was complete.[30−32] A comparison of the oscillator strengths calculated in the different formulations thus gives a measure of the completeness of the computational basis in addition to the fulfillment of the TRK sum rule (vide infra).

4. Details of the Calculations

To be consistent with our previous work on the two amino acids glycine and alanine,[12,16] we have optimized the geometries of the five nucleobases at the density functional theory (DFT) level with the B3LYP functional[33] and the 6-31+G(d,p)[34] one-electron basis set using the Gaussian program.[35] No searches of different rotamers or conformers were carried out. Instead we started the optimizations from geometries which had already been optimized at the MP2/6-31G* level.[36] After the geometry optimization the molecules were reoriented in such a way that the heterocycles are placed in the *xy*-plane as shown in Figures 1 and 2.

Once the minimum energy molecular geometries of the nucleobases were established, vertical singlet excitation energies and associated electronic transition dipole moments were calculated with the TURBOMOLE program[37,38] using linear response or polarization propagator methods[24] at the level of the RPA. As the cc-CVTZ+(3df,p)&s+p+d-recontracted basis developed for glycine[12] produced excellent results for that amino acid (see Table 1 of ref 12 for details), we chose to use the same basis also for the present calculations.[39] Preliminary calculations were also carried out at the level of time-dependent density functional theory (TDDFT)[40,41] employing the Perdew−Burke−Ernzerholf (PBE) functional.[42] However, the results differed by less than 1% from the RPA results in line with our previous comparisons,[14,16] and in the following we will only report results of calculations carried out at the RPA level.

As noted above, in the complete basis set limit of the RPA the TRK sum rule should be equal to the number of electrons N_e, and the mean excitation energies calculated from oscillator strengths in the length, mixed, or velocity representation should have the same values. The adherence to eq 6 and the agreement between the mean excitation energies in different representations thus provide figures of merit for the basis set used in calculation. In Table 1 we have thus listed the TRK sum rules in the length representation and the mean excitation energies in length and velocity representation. We observe excellent agreement between the length and the velocity representation of the mean excitation energy as well as for the TRK sum rule and can therefore conclude that our tailor-made basis set is not only suitable for the amino acids glycine and alanine,[12,16] but also for the nucleobases sufficiently close to the basis set limit.

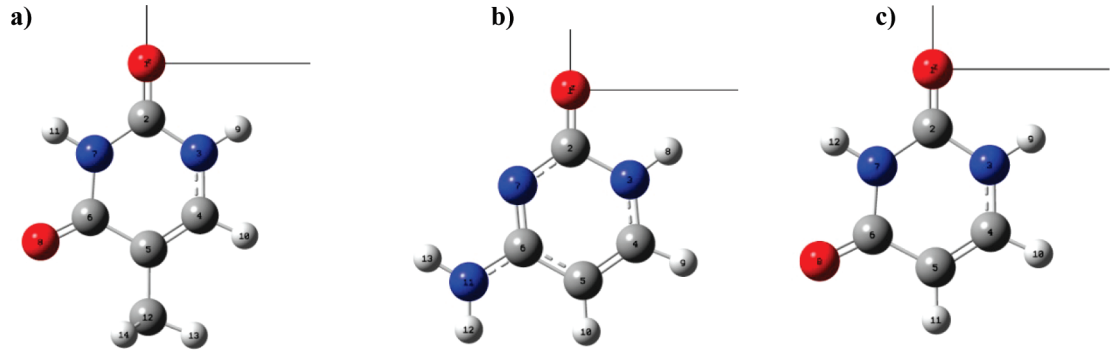

Figure 1. Optimized geometries of the pyrimidine nucleobases thymine (a), cytosine (b), and uracil (c). The molecules lie in the *xy*-plane with the *y*-axis point upward and the *x*-axis to the right.

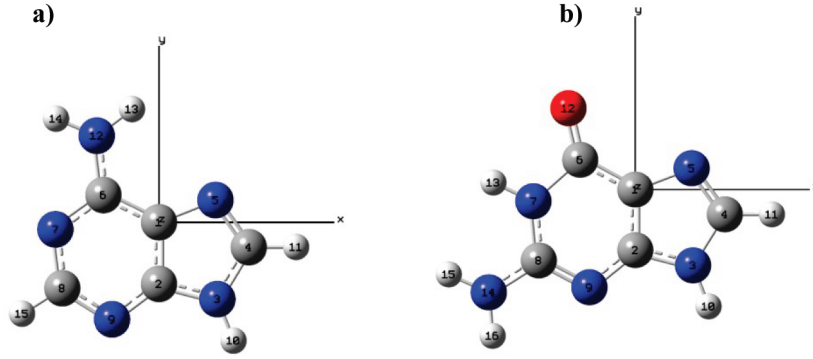

Figure 2. Optimized geometries of the purine nucleobases adenine (a) and guanine (b). The molecules lie in the *xy*-plane as indicated.

TABLE 1: Number of Electrons, TRK Sum Rule in the Length Representation S_0^L, and the Mean Excitation Energy in the Length and Velocity Representation, I_0^L and I_0^V, for the Nucleobases

	N_e	S_0^L	I_0^L (eV)	I_0^V (eV)
cytosine	58	58.00	69.60	69.51
uracil	58	58.03	73.13	73.06
thymine	66	66.01	70.00	69.99
adenine	70	70.01	69.06	69.03
guanine	78	78.05	71.58	71.46

5. The Bragg Rule

Because of the difficulty of calculating the stopping cross section of large molecules,[43] many calculations have been based on the premise that the cross section for an aggregate system may be determined from a weighted sum of the atomic stopping cross sections:

$$S(v)^{\text{aggregate}} = \sum_{i=\text{fragments}} n_i S_i(v) \tag{17}$$

Such a notion that the total stopping cross section can be represented as the sum of its parts is known as the Bragg Rule.[44] One might expect that the Bragg Rule, at least as stated here, cannot be particularly accurate as it represents a molecule as an aggregate of atoms and neglects chemical binding effects. However, guided by chemistry, one might formulate a Bragg Rule for molecular fragments or other aggregates, which includes terms for bonding, and thus recovers the effects of chemical bonding within each fragment. We have implemented this scheme for small molecules in a cores and bonds approach[13,15,45,46] where the mean excitation energies corresponding to specific bonds and atomic cores were calculated and used to determine molecular stopping cross sections. It should also be noted that the molecular mean excitation energy is dominated by the atomic core values, and that bonding effects are small perturbations on the sums of the atomic mean excitation energies.

As the mean excitation energy is simply related to the stopping number (eq 3), it is also possible to write a combination law for fragment mean excitation energies which is consistent with the Bragg Rule. In this case, the mean excitation energy, I_0, for a molecule containing N_e electrons and divided into fragments, each with fragment mean excitation energy I_0^i and associated with ω_i electrons would be:

$$\ln I_0 = \frac{1}{N_e} \sum_{i=\text{fragments}} \omega_i \ln I_0^i \tag{18}$$

This is the formulation that we have used[15] to calculate the mean excitation energies for some amino acids. We will compare the results calculated using a Bragg rule formulation to those obtained from whole molecule calculations on the nucleobases.

6. Mean Excitation Energies of Nucleobases

Using the methodology described in Sections 3 and 4 above, the directional components of the mean excitation energies, the isotropically averaged mean excitation energies, and the anisotropies for the five nucleobases are given in Table 2, along with similar quantities for the amino acids glycine and alanine for comparison.

The initial observation concerning the isotropic mean excitation energies is that they do not differ among the nucleobases by more than a few percent. This is a consequence of the fact that all of the bases have a similar electronic structure. They are made up of the same sorts of atomic cores and chemical bonds. They all contain many electrons ($N > 55$), so small

TABLE 2: Components and Anisotropy of the Mean Excitation Energy for the Nucleobases in Length Representation in Comparison with Values for Glycine and Alanine (from Ref 16)

	I_0 (eV)	I_0^x (eV)	I_0^y (eV)	I_0^z (eV)	A
cytosine	69.60	66.10	62.65	81.26	27.06
uracil	73.13	68.72	66.97	84.86	25.97
thymine	70.00	66.92	63.43	80.73	28.30
adenine	69.06	62.63	64.34	81.84	35.57
guanine	71.58	64.62	67.03	84.51	39.01
glycine[16]	71.10	69.12	67.73	76.77	9.21
alanine[16]	67.37	65.91	65.45	70.88	7.32

differences in the oscillator strength distribution are minimized by the large denominator in eq 4. Another way of interpreting this is related to the fact that for increasingly large molecules the density of states in the continuum, which, for example, in alanine contributed almost 90% to the mean excitation energy,[16] becomes so dense that adding additional atoms will not make a significant difference.

In comparison, the amino acids, glycine and alanine, are considerably smaller, with less than 50 electrons, so that the small differences in electronic structure are not as easily obscured. In very small systems, such as C_2HO ($N = 26$), electronic structure and chemical bonding effects become more important, and the differences in mean excitation energies between isomers such as Me_2O and EtOH are meaningful.[47] Indeed, the interpretation given here is much in line with using a Bragg-like cores and bonds sum rule.[15] Using the core and bond mean excitation energies from ref 15 in eq 18, we find isotropic mean excitation energies for uracil and adenine of 80.83 and 69.73 eV, respectively, about the accuracy that one might expect from such an approximation.

Although there has been no systematic experimental study of the mean excitation energies of the nucleobases, experimental values of 71.40 and 75.00 eV have been reported[48] for adenine and guanine, respectively, in reasonable agreement with our results as reported in Table 2. There is also a set of mean excitation energies calculated for the nucleobases using a dielectric model and an evaluation of the optical energy loss function.[49] Those results are somewhat larger than the ones obtained here, with an average mean isotropic excitation energy of 75.25 eV as opposed to the average over the five nucleobases of 70.67 eV calculated here, which is an acceptable agreement.

Although the nucleobases have very similar isotropic mean excitation energies, thus all having similar propensities to absorb energy from a swift ion, they differ significantly in their directional mean excitation energies; that is, the mean excitation energies differ when the target molecule has a specific orientation with respect to the projectile beam.

It can be shown[22] that electronic excitations in a target molecule can only occur in directions perpendicular to the direction of projectile motion. In the work reported here, the nucleobases are placed in the *xy*-plane. For the nucleobases, the mean excitation energy is quite anisotropic, and in all cases I_0^z is considerably ($\sim 30\%$) larger than either I_0^x or I_0^y, which are approximately equal for the bases. Thus projectiles traveling perpendicular to the molecular plane are expected to deposit much less energy into the target base than projectiles traveling in the molecular plane. This is most certainly a reflection of the greater time in contact with the target electron density for a projectile traveling parallel to the molecular plane.

The anisotropy of the purine nucleobases is larger than that of the pyrimidine, which is attributable to the larger physical extension in the direction of the molecular plane. The mean excitation energy of the nucleobases is more anisotropic than in the case of the amino acids, which is caused by the fact that the nucleobases include planar heterocycles with conjugated π-bonds.

TABLE 3: Mean Excitation Energies of Some Hydrogen-Bonded Species

system	I_0 (eV)
H_2O	73.56
$(H_2O)_2$	73.18
NH_3	55.25
$(NH_3)_2$	54.89
H_2O-NH_3	63.24

The most interesting aspects of the radiation biology of the nucleobases come, however, when they are pairwise hydrogen-bonded as in RNA or DNA or combined with ribose to form nucleotides or nucleosides. We consider each of these situations.

7. Hydrogen Bonding

In either the conventional Watson−Crick or Hoogsteen base pairing in DNA or RNA, base pairs are combined with two (adenine−thymine in DNA or adenine−uracil in RNA) or three (guanine−cytosine) hydrogen bonds. Although these hydrogen-bonded systems have been studied computationally,[50] the effect of hydrogen bonding on mean excitation energy is not known. The effect of hydrogen bonds was investigated not for the base pairs in this work, as this would require prohibitively extensive calculations. However, in accordance with the discussion above, we expect to see the largest effect arising from hydrogen-bond formation in smaller complexes. As the hydrogen bonds among nucleobases all involve O and N, we have therefore investigated the water and ammonia dimers as well as a water−ammonia complex.

Using the same basis sets and methods described above, the mean excitation energies of water, ammonia, and their hydrogen-bonded pairs were calculated. They are given in Table 3. The complex geometries were determined by energy minimization. The mean excitation energies are in excellent agreement with previous calculations,[11] which found the mean excitation energies of water and ammonia to be 73.31 and 55.24 eV, respectively.

Table 3 shows that the calculated mean excitation energies of the water dimer and the ammonia dimer are smaller only by less than a percent from those of the monomers. Similarly, the calculation of a mean excitation energy using a Bragg-like rule [$\ln I_{H_2O/NH_3} = 1/20(10 \ln I_{H_2O} + 10 \ln I_{NH_3})$] for the mixed dimer, H_2O-NH_3, gives a result of 63.75 eV. Using this as the analogue of the non-hydrogen-bonded system, again hydrogen bonding only slightly reduces the mean excitation energy of the molecules. Since one would expect that any effect of hydrogen bonding on the mean excitation energy would be larger in small molecules (vide supra), we conclude that hydrogen bonding will not change the mean excitation energies of the nucleobases significantly.

8. Nucleosides

Nucleosides are the next step in complexity after the nucleobases and, along with phosphates, make up nucleotides, or the structural units of RNA and DNA. A nucleoside is a combination of a nucleobase connected to a ribose, a five-carbon cyclic sugar ($C_5O_5H_{10}$). Although we have not calculated the mean excitation energy of the nucleosides directly, because of the computational requirements of such a calculation, we can

TABLE 4: Mean Excitation Energies of Five Nucleosides

nucleoside	I_0 (eV)
cytidine	69.96
uridine	71.41
methyl uridine	70.12
adenosine	69.68
guanosine	70.89

estimate the effect on the mean excitation energy of a nucleobase using the cores and bonds approach mentioned above[15] (eq 18). Using a Bragg Rule fragment approach[15] one can write an equation for the mean excitation energy of a nucleoside (I_{NS}) in terms of the mean excitation energy of a ribose fragment missing an −OH group ($I_{R'}$), the mean excitation energy of the parent nucleobase (I_{NB}), and the number of electrons in the nucleobase (N):

$$\ln I_{NS} = \frac{1}{72 + N}[80 \ln I_{R'} + (N - 4) \ln I_{NB} - 4 \ln I_{N-H}] \quad (19)$$

The results using this approach for the five nucleosides are presented in Table 4.

Again, as with hydrogen bonding, forming the nucleoside from the nucleobase has little effect on the mean excitation energy of the system.

9. Summary

We conclude that biological material has a very stable mean excitation energy of approximately 70 eV under many circumstances. Previous work has shown that amino acids have very similar mean excitation energies regardless of small geometry changes or even whether they are found in neutral or zwitterions form.[12] Similarly, a better treatment of electron correlation via different DFT functionals[16] as well as inclusion of the effects of surrounding water molecules via a solvent QM/MM calculation[14] did not show significant effects. In the calculations reported here, we also see that neither hydrogen bonding[51] nor formation of nucleosides significantly alters the mean excitation energy of these biomolecules. Further, water has nearly the same mean excitation energy as do the nucleobases (73.31 eV[11]), making it difficult to use swift ion radiation as a tool to manipulate single nucleobases.

Finally, the stability and consistency of the mean excitation energy of biological material explains why the Bragg Rule, either atomic or cores and bonds, works well for these systems.

Acknowledgment. This work was supported by grants from the Danish Center for Scientific Computing, the Carlsberg foundation, and the Danish Natural Science Research Council/ The Danish Councils for Independent Research (SPAS).

Note Added after ASAP Publication. This manuscript was published on the Web on June 2, 2010. Updates were made to equation numbering. The corrected version was reposted on October 8, 2010.

References and Notes

(1) Sisterson, J. *Nucl. Instrum. Methods Phys. Res., Sect. B* **2005**, *241*, 713.
(2) Amaldi, U.; Kraft, G. *Rep. Prog. Phys.* **2005**, *68*, 1861.
(3) Zhang, W.; Muirhead, C. R.; Hunter, N. *J. Radiol. Prot.* **2005**, *25*, 393.
(4) Ruhm, W.; Walsh, L.; Chomentowski, M. *Radiat. Environ. Biophys.* **2003**, *42*, 119.
(5) von Sonntag, C. *The Chemical Basis for Radiation Biology*; Taylor and Francis: London, 1987.
(6) von Sonntag, C. *Free-radical DNA damage and its repair - a chemical perspective*; Springer Verlag: Heidelberg, 2005.
(7) Schlathölter, T.; Alvardo, F.; Hoekstra, R. *Nucl. Instrum. Methods Phys. Res., Sect. B* **2005**, *233*, 62.
(8) Bethe, H. *Ann. Phys. (Leipzig)* **1930**, *5*, 325. *Z. Phys.* **1932**, *76*, 293. *Phys. Rev.* **1953**, *89*, 1256.
(9) Bonderup, E. *Penetration of Charged Particles through Matter*, 2nd ed.; Fysik Instituts Trykkeri, Aarhus Universitet: Arhus, Denmark, 1981.
(10) Sauer, S. P. A.; Sabin, J. R.; Oddershede, J. *Phys. Rev. A* **1993**, *47*, 1123–1129.
(11) Sauer, S. P. A.; Sabin, J. R.; Oddershede, J. *Nucl. Instrum. Methods Phys. Res., Sect. B* **1995**, *100*, 458–463.
(12) Sauer, S. P. A.; Oddershede, J.; Sabin, J. R. *J. Phys. Chem. A* **2006**, *110*, 8811–8817.
(13) Sabin, J. R.; Oddershede, J.; Sauer, S. P. A. *AIP Conf. Proc.* **2008**, *1080*, 138–144.
(14) Adias, K.; Kongsted, J.; Sabin, J. R.; Oddershede, J.; Mikkelsen, K. V.; Sauer, S. P. A. *J. Phys. Chem. Lett.* **2010**, *1*, 242–245.
(15) Bruun-Ghalbia, S.; Sauer, S. P. A.; Oddershede, J.; Sabin, J. R. *J. Phys. Chem. B* **2010**, *144*, 633–637.
(16) Bruun-Ghalbia, S.; Sauer, S. P. A.; Oddershede, J.; Sabin, J. R. *Eur. Phys. J. D*, DOI: 10.1140/epjd/e2010-00034-7.
(17) Ziegler, J. F.; Biersack, J. P. Littmark, U. *The Stopping and Range of Ions in Solids. Vol. 1 of the Stopping and Ranges of Ions in Matter*; Pergamon Press: Oxford, 1985.
(18) Janni, J. F. *At. Data Nucl. Data Tables* **1982**, *27*, 147.
(19) Thomas, W. *Naturwiss.* **1925**, *13*, 627.
(20) Kuhn, W. *Z. Phys.* **1925**, *33*, 408–412.
(21) Reiche, F.; Thomas, W. *Z. Phys.* **1925**, *34*, 510–525.
(22) Mikkelsen, H. H.; Oddershede, J.; Sabin, J. R.; Bonderup, E. *Nucl. Instrum. Methods Phys. Res., Sect. B* **1995**, *100*, 451–457.
(23) Inokuti, M.; Karstens, W.; Shiles, E.; Smith, D. Y. *Mean Excitation Energy for the Stopping Power of Silicon from Oscillator-Strength Spectra*. Presented at the 2005 APS March Meeting, Los Angeles, California, March 21−25, 2005; http://meetings.aps.org/link/BAPS.2005.MAR.R1.55 (accessed Dec 4, 2009).
(24) For a review of the theory and implementation of the polarization propagator method, see: Oddershede, J.; Jørgensen, P.; Yaeger, D. L. *Comput. Phys. Rep.* **1984**, *2*, 33. Oddershede, J. *Adv. Chem. Phys.* **1987**, *69*, 201. Sauer, S. P. A.; Packer, M. J. The Ab Initio Calculation of Molecular Properties Other than the Potential Energy Surface. In *Computational Molecular Spectroscopy*; Bunker, P. R., Jensen, P., Eds.; John Wiley and Sons: London, 2000; Chapter 7; pp 221−252.
(25) Geertsen, J.; Oddershede, J.; Sabin, J. R. *Phys. Rev. A* **1986**, *34*, 1104.
(26) Jørgensen, P.; Oddershede, J.; Beebe, N. H. F. *J. Chem. Phys.* **1978**, *68*, 2527.
(27) Sauer, S. P. A.; Diercksen, G. H. F.; Oddershede, J. *Int. J. Quantum Chem.* **1991**, *39*, 667–679.
(28) McLachlan, A. D.; Ball, M. A. *Rev. Mod. Phys.* **1964**, *36*, 844.
(29) Rowe, D. J. *Rev. Mod. Phys.* **1968**, *40*, 153.
(30) Hansen, A. E.; Bouman, T. D. *Mol. Phys.* **1979**, *37*, 1713.
(31) Harris, R. A. *J. Chem. Phys.* **1969**, *50*, 3947.
(32) Jørgensen, P.; Oddershede, J. *J. Chem. Phys.* **1983**, *78*, 1898.
(33) Lee, C.; Yang, W.; Parr, R. G. *Phys. Rev. B* **1988**, *37*, 785. Becke, A. D. *J. Chem. Phys.* **1993**, *98*, 5648.
(34) Hehre, W. J.; Ditchfield, R.; Pople, J. A. *J. Chem. Phys.* **1972**, *56*, 2257. Clark, T.; Chandrasekhar, J.; Schleyer, P. *J. Comput. Chem.* **1983**, *4*, 294.
(35) Frisch, M. J. et al. *Gaussian 03*, Revision B.05; Gaussian, Inc.: Pittsburgh, PA, 2003.
(36) Schreiber, M.; Silva-Junior, M. R.; Sauer, S. P. A.; Thiel, W. *J. Chem. Phys.* **2008**, *128*, 134110.
(37) Ahlrichs, R.; Bär, M.; Häser, M.; Horn, H.; Kölmel, C. *Chem. Phys. Lett.* **1989**, *162*, 165. Häser, M.; Ahlrichs, R. *J. Comput. Chem.* **1989**, *10*, 104. Treutler, O.; Ahlrichs, R. *J. Chem. Phys.* **1995**, *102*, 346. Bauernschmitt, R.; Ahlrichs, R. *Chem. Phys. Lett.* **1996**, *256*, 454. Grimme, S.; Furche, F.; Ahlrichs, R. *Chem. Phys. Lett.* **2002**, *361*, 321. Furche, F.; Rappoport, D. Computational Photochemistry. In *Computational and Theoretical Chemistry*; Olivucci, M., Ed.; Elsevier: Amsterdam, 2005; Vol. 16; Chapter 3. Arnim, M. V.; Ahlrichs, R. *J. Chem. Phys.* **1999**, *111*, 9183.
(38) *TURBOMOLE V6.0 2009*, University of Karlsruhe and Forschungszentrum Karlsruhe GmbH, 1989−2007, TURBOMOLE GmbH, since 2007; http://www.turbomole.com.
(39) The orbital exponents and contraction coefficients for the basis are given in Tables 2−5 of ref 12.
(40) Runge, E.; Gross, E. K. U. *Phys. Rev. Lett.* **1984**, *52*, 997.
(41) Schirmer, J.; Dreuw, A. *Phys. Rev. A* **2007**, *75*, 022513.

(42) Perdew, J. P.; Burke, K.; Ernzerhof, M. *Phys. Rev. Lett.* **1996**, *77*, 3865–3868.

(43) Sabin, J. R.; Oddershede, J. *Nucl. Instrum. Methods Phys. Res., Sect. B* **1992**, *64*, 678.

(44) Bragg, W. H.; Kleeman, R. *Philos. Mag.* **1905**, *10*, 318.

(45) Sabin, J. R.; Oddershede, J. *Nucl. Instrum. Methods Phys. Res., Sect. B* **1987**, *27*, 280.

(46) Oddershede, J.; Sabin, J. R. *Nucl. Instrum. Methods Phys. Res., Sect. B* **1989**, *42*, 7.

(47) Sabin, J. R.; Oddershede, J. *Nucl. Instrum. Methods Phys. Res., Sect. B* **1992**, *64*, 678.

(48) U.S. National Institute of Standards and Technology ASTAR database; http://physics.nist.gov/cgi-bin/Star/compos.pl?175 (accessed March 1, 2010).

(49) Tan, Z.; Xia, Y.; Zhao, M.; Liu, X. *Nucl. Instrum. Methods Phys. Res., Sect. B* **2006**, *248*, 1.

(50) Kryachko, E. E.; Sabin, J. R. *Int. J. Quantum Chem.* **2003**, *91*, 695.

(51) Ratner, M. Strong-Coupling Model for the Analysis of Spectral Properties of Hydrogen-Bonded Systems. Ph.D. Thesis, Northwestern University, Evanston, IL, 1969.

JP1021054